



New method for revealing dislocations in garnet: premelting decoration

Xiangwen Liu^{1,2} · Zhanjun Xie^{2,3} · Zhenmin Jin^{2,3} · Zhuoyue Li³ · Ping Ao³ · Yikun Wu³

Received: 19 February 2018 / Accepted: 30 April 2018 / Published online: 17 May 2018
© Springer-Verlag GmbH Germany, part of Springer Nature 2018

Abstract

Premelting decoration (PMD) of dislocation experiments was carried out on garnets at 1 atmosphere pressure and temperatures of 800–1000 °C. Numerous decorated lines were observed on the polished surface of heat-treated garnet grains. The results of scanning electron microscopy, laser Raman spectroscopy and transmission electron microscopy (TEM) analyses indicate that these decorated lines were generated by premelting reaction along the dislocation lines and subgrain boundaries. The constituents of decorated lines on the polished surface of garnet are hematite, magnetite, and melt. While, in the interior of garnet, their constituents changed to Al-bearing magnetite and melt. The dislocation density of a gem-quality megacrystal garnet grain by means of the PMD is similar to that obtained by TEM, which confirms that the PMD is a new reliable method for revealing dislocations in garnet. This method greatly reduces the cost and time involved in the observation of dislocation microstructures in deformed garnet.

Keywords Garnet · Dislocation decoration · Premelting · TEM

Introduction

Garnet is an important constituent mineral in eclogite and other crustal, as well as upper mantle rocks (Baxter et al. 2013). The results of deformation experiments show that garnet can be deformed plastically at high-pressure and -temperature conditions, and its creep strength and brittle–ductile transition temperature are significantly higher than most of silicate minerals (Jin et al. 2001; Karato et al. 1995; Mei et al. 2010; Voegelé et al. 1998a; Wang and Ji 1999; Xu et al. 2013). Hence, the ductility of natural garnet provides information on the geodynamic processes in the lower crust and the upper mantle and, especially, in the subduction zones (Caddick and Kohn 2013; Ji and Martignole

1994; Voegelé et al. 1998b). However, as garnet is an isotropic mineral, it is difficult to examine its plastic deformation microstructures by optical microscope. Fortunately, the dislocation pattern of garnet can reflect its deformation conditions (Ando et al. 1993; Carstens 1969; Chen et al. 1996; Doukhan et al. 1994; Lü et al. 2004; Prior et al. 2000). To date, there are two commonly used methods to observe the dislocation microstructures of garnet: (1) transmission electron microscopy (TEM) for high-resolution analysis (Allen et al. 1987): TEM observations have some shortcomings on large area and in situ analysis of unevenly distributed dislocations (Prior et al. 2000; Voegelé et al. 1998b). (2) Etch pitting with hydrofluoric acid at the crystal surface (Carstens 1969, 1971; Voegelé et al. 1998a): this method is just suitable for Mg-rich garnet, which indicates that this etching reaction is controlled by chemical compositions of crystal (Ji and Martignole 1994). As the other method, the orientation contrast imaging with electron backscatter diffraction (EBSD) is effective for revealing subgrain boundaries, but it has not been proven to be useful in analyzing free dislocations (Massey et al. 2011; Smit et al. 2011). While the electron channeling contrast imaging (ECCI) with EBSD is a potentially powerful technique to analyze the free dislocations in garnet (Gutierrez-Urrutia and Raabe 2012; Kleinschrodt and McGrew 2000; Zhang et al. 2015), but it is an

✉ Xiangwen Liu
xwliu@cug.edu.cn

¹ Engineering Research Center of Nano-Geo Materials of Ministry of Education, China University of Geosciences, Wuhan 430074, China

² State Key Laboratory of Geological Processes and Mineral Resources, China University of Geosciences, Wuhan 430074, China

³ School of Earth Sciences, China University of Geosciences, Wuhan 430074, China

expensive and complex method. Therefore, the quantitative studies on the geodynamic implications of deformed garnets are still sparse (Ando et al. 1993; Chen et al. 1996; Lü et al. 2004). As the result, new method for observing the dislocation microstructures of garnet is needed.

The well-established method of oxidation decoration of dislocations in olivine (Jung et al. 2014; Karato 1987; Kohlstedt et al. 1976) encouraged us to explore a similar method applying the garnet grain. Furthermore, the crystal premelting, a process that melting preferentially occurs at the highly strained regions, such as dislocation lines and (sub)grain boundaries, below the thermodynamically calculated melting temperatures (Alsayed et al. 2005; Bartis 1977; Gómez et al. 2003; Hand and Dirks 1992; Mei and Lu 2007; Tumarkina et al. 2011), can be regarded as marks of mineral crystal defects (Levine et al. 2016). The previous studies found that the garnet end members of almandine and grossular would begin to decompose directly into melt with or without other crystalline phases present at ~ 800 °C under low-pressure conditions (Hsu 1968; Keesmann et al. 1971), even though their melting temperatures (T_m) are above 1000 °C (Karato et al. 1995). In this paper, we investigated the premelting phenomenon at the crystal defects of garnet at 1 atmosphere pressure and temperatures of 800–1000 °C, and propose that it is an effective new method for decorating the dislocation microstructures in garnet.

Sample description and experimental procedure

The garnet samples in this study were selected from one eclogite sample and one gem-quality megacrystal garnet. The eclogite sample Hcc4-1 was collected from the Shuanghe ultrahigh pressure (UHP) metamorphic terrane, which is part of the Dabie orogenic belt of China. There have been many detailed geological, petrological and geochemical studies about this area, which show that the age of peak metamorphism is 226–234 Ma at pressures of above 2.7 GPa and temperatures of 700–850 °C (Cong et al. 1995; Li et al. 2000; Liou et al. 1997; Liu et al. 2006; Okay 1993). The garnet from the eclogite sample is fresh and elongated substantially (Figs. 1a, 2a), which suggests that it underwent plastic deformation. The end members of almandine and grossular account for > 80 wt% of the studied garnet grains in which water content is up to ~ 2500 wt ppm H_2O (Liu et al. 2016). The gem-quality megacrystal garnet Mgc1-1 was collected from Mozambique (Fig. 1b). We used both of our decoration method and TEM analysis to investigate the dislocation characteristics of garnet.

The experiments were carried out in the following steps: (1) the eclogite sample was cut into a $\sim 4 \times 3 \times 1$ cm³ block, which was highly polished on one side (Fig. 1a).

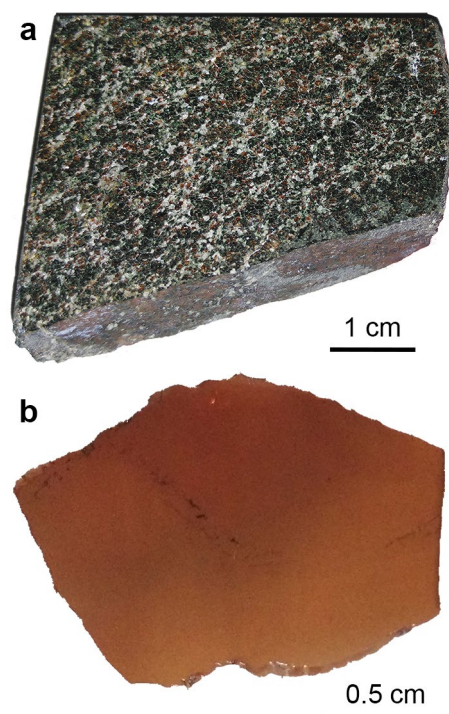
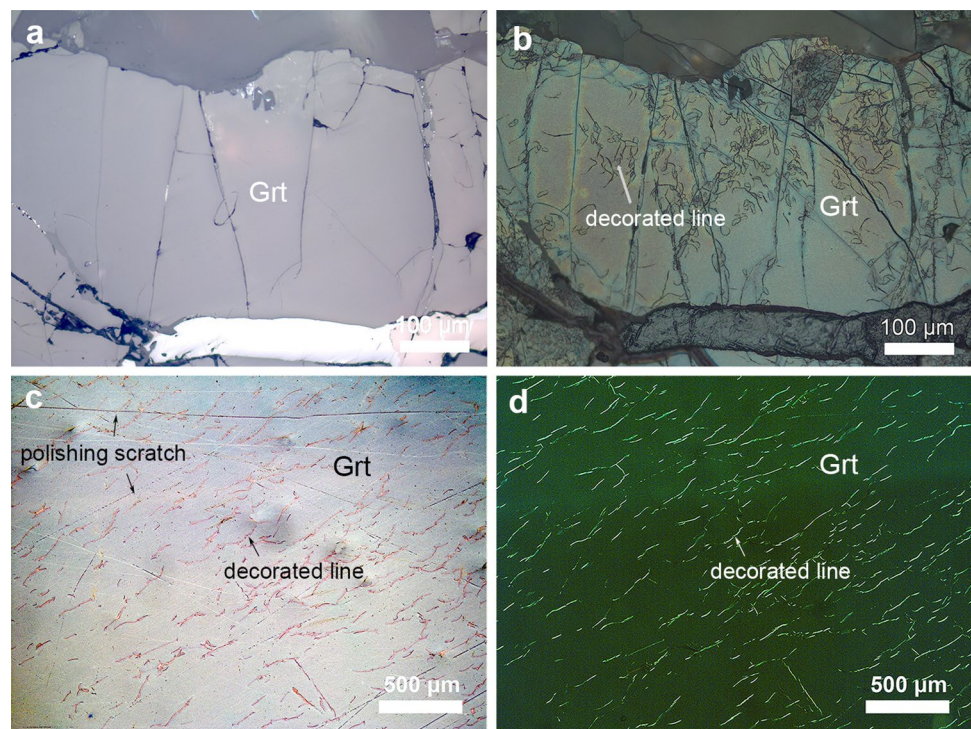


Fig. 1 **a** Single-sided polished block of the eclogite sample Hcc4-1. **b** Double-sided polished section of the megacrystal garnet Mgc1-1

The megacrystal garnet was prepared as a doubly polished, ~ 0.5 -mm-thick section (Fig. 1b). (2) The microstructures on the polished side of the garnets were photographed by an optical microscope. (3) Since the decomposition temperature of almandine and grossular, which are the main end members of garnets from Shuanghe eclogite (Liu et al. 2016), is ~ 800 °C under low-pressure conditions (Hsu 1968; Keesmann et al. 1971), the prepared samples were heated using an open muffle furnace to 800 °C with a rate of 2°C/min. Then, the samples were cooled to room temperature just after reaching the setting temperatures. In addition, we also heated the eclogite sample Hcc4-1 in nitrogen atmosphere to check the effect of oxygen fugacity (f_{O_2}) on the decorating phenomenon of garnet. (4) After the heat treatment at desired temperature, the polished surface was examined by an optical microscope. If the garnet grains do not show decorated lines, the target temperature of heat treatment will be increased by 10 °C. Such heating and cooling cycles would be continued until the decorated lines become easy to be identified under reflected light. (5) The decorated lines were investigated using a combination of SEM, LRS, and TEM at the State Key Laboratory of Geological Processes and Mineral Resources (GPMR).

The microstructures of heat-treated garnet grains were observed using a Quanta 450 FEG-SEM. The Raman spectra were obtained on a Renishaw RM-1000 LRS system. The 532-nm line of Ar⁺ laser at 20 mW was used for sample

Fig. 2 **a, b** Photomicrographs (reflected light) of the same garnet grain's polished surface in the eclogite block Hcc4-1 before and after cyclic heat treatment to 970 °C, respectively. The numerous dark decorated lines are observed only in **b**. Photomicrographs of the decorated lines in the same area of megacrystal garnet Mgc1-1 after cyclic heat treatment to 980 °C, taken by reflected light (c) and cross-polarized light (d)



excitation (corresponding to 2 mW on the sample). Both the spectral resolution and the accuracy in the Raman shift were estimated to be $\pm 1 \text{ cm}^{-1}$. The TEM samples were processed by a Gatan 656 dimple grinder, a Gatan-600 ion mill, and a JEOL-JEE4X vacuum evaporator for physical thinning, ion thinning and carbon coating, respectively. The chemical composition and microstructures of the decorated lines were determined by a Philips CM12 TEM, which was equipped with an EDAX PV9100 X-ray energy-dispersive spectroscope (EDS) and a Gatan 830 charge-coupled device (CCD) camera system. Observations were made at an accelerating voltage of 120 kV with a point-to-point resolution of 0.34 nm and a line resolution of 0.2 nm.

Experimental results

Decorated lines of garnet under the optical microscope

By comparing the photomicrographs taken by reflected light of each heat treatment experiment, we found that the first occurred temperatures of decorated lines on the polished surface of garnet grains are around 950 °C. As the heating temperature increases, the decorated lines become darker in color and wider in width and reach the best contrast with the matrix at 970–980 °C. As shown in Fig. 2b, when the heat treatment temperature reaches 970 °C, numerous dark decorated lines can be observed clearly on the polished surface

of garnet grains in the eclogite block Hcc4-1 under reflected light. These decorated lines exhibit heterogeneous distribution characteristics, and most of them appear as small curves and loops distributing in the core area of the polished surface of garnet grains. In contrast, the decorated lines in the megacrystal garnet Mgc1-1 are short and straight, and their distribution is generally homogeneous (Fig. 2c, d).

Microstructures and compositions of the decorated lines

The microstructures and compositions of the decorated lines in the studied garnets were analyzed by SEM, LRS, and TEM. The decorated lines in the garnet grains are clear and bright in the backscattered electron image of SEM (Fig. 3a), indicating that their compositions are dominated by phases with high mean atomic number. The secondary electron image shows that the shape of these lines bulge out of the polished surface (Fig. 3b). This bulging nature could scatter the light, leading to a dark color appearance under the reflected light (Fig. 2b, c).

As shown in Fig. 4 and Table 1, compared with the garnet before heat treatment, the Raman spectra indicate that there are some new phases generating in the heat-treated garnet grains. The peaks around 351, 502, 552 and 906 cm^{-1} in all spectra are assigned to a solid solution of almandine and grossular (Gillet et al. 1992). The Raman spectrum of decorated line on the polished surface of garnet heated in air (Fig. 4a) indicates that it is a mixture of iron oxides and

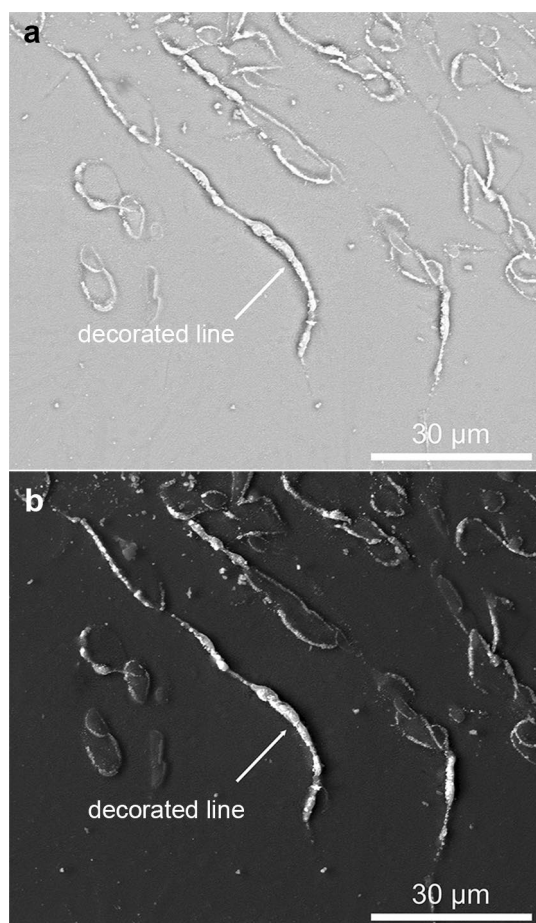


Fig. 3 **a** Backscattered electron image and **b** secondary electron image of the decorated lines in the garnet from the eclogite sample Hcc4-1. The bright color and bulging nature of decorated lines strongly suggest that their compositions are dominated by the volume expanded phases with high mean atomic numbers

garnet. The peaks at 224, 243, 291, 409, 502 and 615 cm^{-1} agree well with the reported data of hematite (De Faria and Lopes 2007; De Faria et al. 1997). The peak at 667 cm^{-1} is assigned to the A_{1g} mode of magnetite (Shebanova and Lazor 2003; Thibeu et al. 1978). But the spectrum of decorated line in the interior of garnet after heated in air (Fig. 4b) shows that there is no hematite composition and the A_{1g} mode peak of magnetite has shifted to 689 cm^{-1} (D’Ippolito et al. 2015; Verble 1974), which is similar to the spectrum of decorated line on the polished surface of garnet heated in nitrogen atmosphere (Fig. 4c).

The dislocation microstructures in garnet within eclogite samples from the same studied area have been analyzed using TEM (Xie et al. 2018), and the results show that the free dislocations and subgrain boundaries (e.g., dislocation arrays, networks, and walls) are widely distributed in garnet grains. However, the present TEM study shows that the microstructures in the interior of heated garnet grains from the eclogite sample Hcc4-1 have been changed. We have not observed the typical free dislocation and subgrain boundary microstructures in the heated garnet grains, but only found numerous small decorated lines exhibiting as pseudomorph after dislocation and subgrain boundary textures. At the middle of decorated lines, numerous microcrystals are assembled as a narrow belt with accompanying gray belts on both sides (Fig. 5a). The selected area electron diffraction patterns and the X-ray energy-dispersive spectra (Fig. 5b) from these microcrystals and gray belts suggest that they are Al-bearing magnetite and Si- and Ca-rich amorphous phase (AP), respectively. The distribution features of these amorphous phases suggest that they are the quenched melt after heat treatment, which is the evidence of partial melting occurring in the heated garnet. Since our garnet was heated below its melting temperature, this partial melting should

Fig. 4 Raman spectra of garnet in the eclogite sample Hcc4-1 before and after heat treatment. **a, b** The spectrum of decorated line on the polished surface and in the interior of garnet after heated in air, respectively. **c** The spectrum of decorated line on the polished surface of garnet after heated in nitrogen atmosphere. **d** The spectrum of garnet before heat treatment. Hem hematite, Mag magnetite and Grt garnet

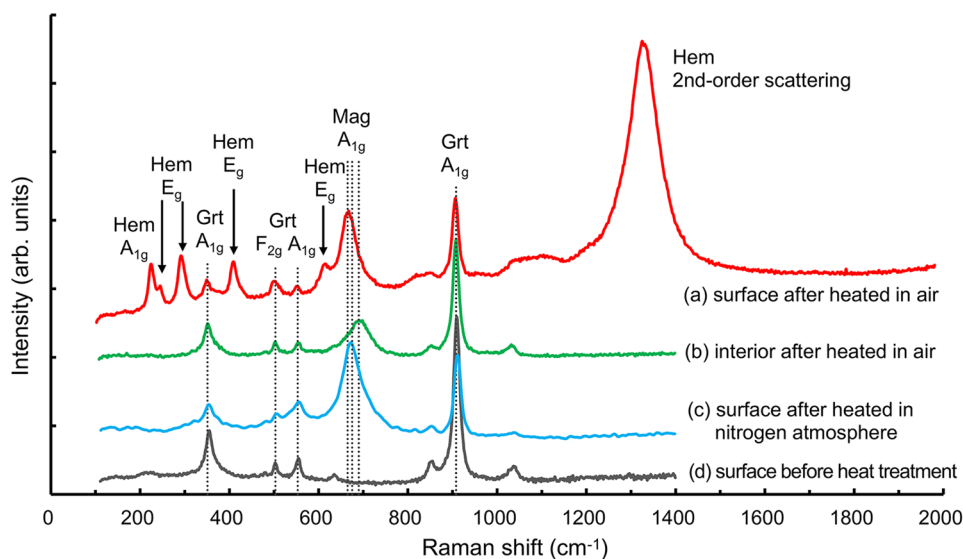


Table 1 Raman mode frequencies (cm^{-1}) of garnet in the eclogite sample Hcc4-1 before and after heat treatment

Spot Modes	Hem A_{1g}	Hem E_g	Hem A_{1g}	Grt A_{1g}	Hem E_g	Grt F_{2g}	Grt A_{1g}	Hem E_g	Mag A_{1g}	Grt A_{1g}	Hem Second-order scattering
<i>a</i>	224	243	291	351	409	502	552	615	667	906	1325
<i>b</i>				351		503	554		689	908	
<i>c</i>				351		503	555		673	909	
<i>d</i>				353		502	554			909	

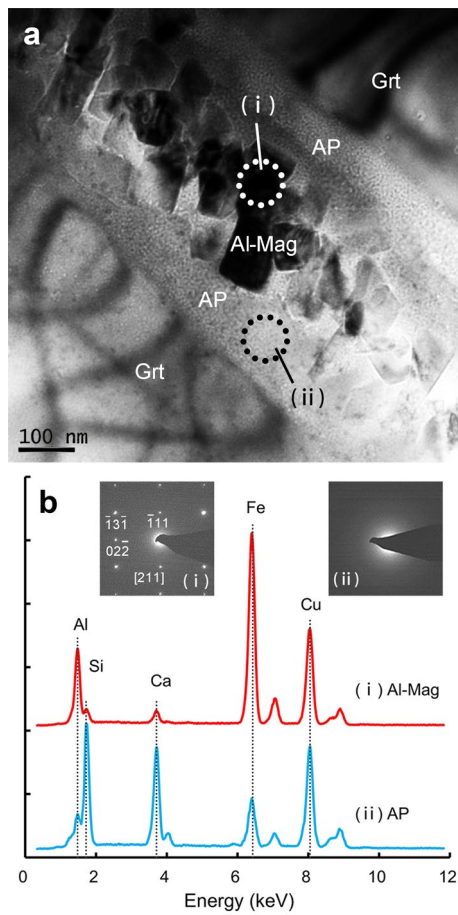


Fig. 5 **a** TEM micrograph of the decorated line in the interior of garnet from the eclogite sample Hcc4-1. **b** The selected area electron diffraction patterns and X-ray energy-dispersive spectra from the dotted encircled regions in **a**. The peaks of Cu in **b** are caused by the TEM specimen holder. *Al-Mag* Al-bearing magnetite and *AP* amorphous phase

belong to the premelting phenomenon (Alsayed et al. 2005; Bartis 1977). The presence of melt with larger volume might be the reason why the shape of decorated lines bulges out of the polished surface (Fig. 3b).

Dislocation density of the megacrystal garnet

Based on the distribution and morphology of the decorated lines in the megacrystal garnet Mgc1-1 (Fig. 2c, d), we infer that these lines are decorated dislocations. The density of these decorated dislocation lines, like that analyzed by TEM, can be simply estimated by the total number (*N*) of dislocations in the measured area (*A*) (Ando et al. 1993; Yamamoto et al. 2017). The estimated result shows that the dislocation density in Fig. 2c is $1.9 \times 10^4 \text{ cm}^{-2}$ (Table 2). On the other hand, since the true definition of dislocation density is the total length (*L*) of all dislocations in a unit volume (*V*) of a crystalline material, we calculated the sample volume corresponding to Fig. 2d based on its area and the thickness of this heated megacrystal garnet section and measured the total length of its decorated dislocations using the ImageJ image-process software (Jung and Karato 2001; Karato and Jung 2003). Based on this calculation method, we obtained a dislocation density of $1.7 \times 10^4 \text{ cm}^{-2}$ in Fig. 2d, which is almost equal to the value based on Fig. 2c. To compare the dislocation microstructures revealed by heat treatment, we also investigated the unheated part of megacrystal garnet Mgc1-1 by TEM. As shown in Fig. 6 and Table 2, only a small number of straight dislocation lines were observed in the TEM specimen yielding a dislocation density of $6.3 \times 10^4 \text{ cm}^{-2}$. Though this value is somewhat higher than that obtained from the optical photomicrographs, they are in the same order of magnitude.

Table 2 Dislocation densities in megacrystal garnet

Sample	Instrument	Mode	Measured area or volume	Dislocation density (10^4 cm^{-2})
Mgc-1 (heated)	Optical microscope	Reflected light	$6,011,381 \mu\text{m}^2$	1.9
		Cross-polarized light	$6,011,381 \times 500 \mu\text{m}^3$	1.7
Mgc-1 (unheated)	TEM	Bright field	$22,344 \mu\text{m}^2$	6.3

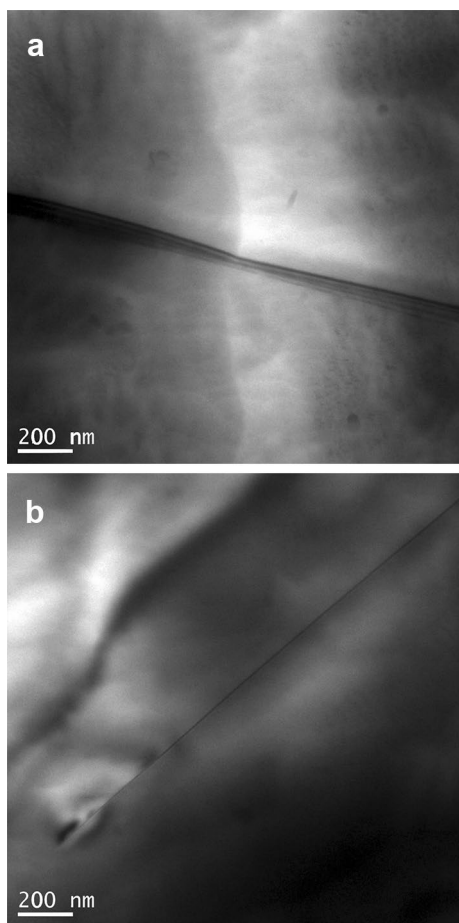


Fig. 6 Dislocation microstructures in the unheated part of the megacrystal garnet

Discussion

Premelting decoration mechanism

Based on the results of SEM, Raman, and TEM analyses, we confirm that the decorated lines observed on the polished surface of heated garnet grains are decorated dislocations or (sub)grain boundaries by premelting reaction. This dislocation decoration mechanism, which can be termed as premelting decoration (PMD), is different from that of oxidation decoration in olivine (Jung et al. 2014; Karato 1987; Kohlstedt et al. 1976).

As illustrated schematically in Fig. 7a, the premelting reaction at crystal defects in garnet under high temperatures can be divided into four stages: (1) before premelting, the crystal defects, such as dislocation lines, exist in garnet grains. (2) Premelting, at high temperatures, the premelting reaction preferentially initiates at the core of dislocations, which causes the crystal around dislocations to decompose directly into melt (Alsayed et al. 2005; Bartis 1977; Hand and Dirks 1992; Mei and Lu 2007; Tumarkina et al. 2011).

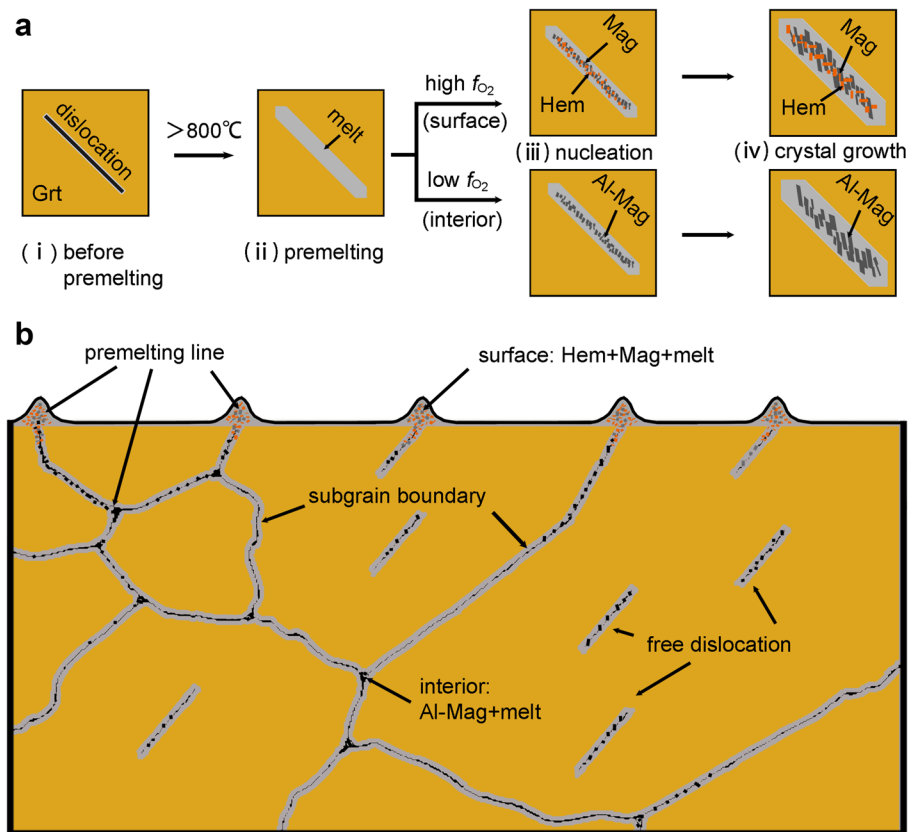
(3) Nucleation, iron oxide minerals nucleate once the garnet premelts. As shown in Fig. 7b, the new products generated by premelting reaction are hematite, magnetite and melt on the polished surface of garnet grains after heated in air. While in the interior of these garnet grains, the new phases are Al-bearing magnetite and melt, which is similar to that on the polished surface of garnet heated in nitrogen atmosphere (Fig. 4). That means the Fe^{3+} content of the premelting products gradually decreases towards the interior of sample, which should be ascribed to the slow oxygen diffusivity (Hsu 1968; Meyers et al. 1980). The presence of Al in magnetite within the garnet interior may account for the shift of its A_{1g} mode peak position from 667 to 689 cm^{-1} (Fig. 4a, b), since the atomic mass of Al^{3+} is lighter than Fe^{3+} (D'Ippolito et al. 2015). The new phases reported here differ somewhat from those reported by Hsu (1968), in which the reaction products are mainly composed of solid solution of magnetite + hercynite and quartz. This difference might be due to the fact that our experiments were carried out at one atmosphere pressure without dwelling at desired temperature, whereas those of Hsu (1968) were performed under high f_{O_2} , below 1 kbar and approximately 900 °C conditions for dozens of hours, which may lead to the incomplete crystallization of quartz. (4) Crystal growth, as temperature increases, the premelting melt belt becomes broader and the crystal size of iron oxide minerals grows bigger. These microcrystals and melts could be preserved and quenched, respectively, during the cooling process of heat treatment, which is the formation mechanism of dislocation pseudomorph textures (Fig. 5a).

Reliability of the premelting decoration method

Previous studies suggest that the decomposition temperatures of silicate garnet range from 750 to 1200 °C, which could change with the factors of chemical composition, temperature, pressure, oxygen fugacity, water content, etc. (Aparicio et al. 2012; Hsu 1968; Keesmann et al. 1971). Therefore, it is very difficult to estimate the optimum temperature for premelting reaction of garnet. However, this is exactly the key point for using the PMD method to reveal dislocation microstructures in garnet. In the present study, the first target temperature of heat treatment is 800 °C, which is the decomposition temperature of the main end members of our garnet (Hsu 1968; Keesmann et al. 1971; Liu et al. 2016). As temperature increases, the premelting decoration lines first occurred at 950 °C and got the best contrast with the matrix at 970–980 °C. Therefore, it can be concluded that the heat treatment by stepwise increasing the target temperature from the decomposition temperature is the ideal procedure for revealing dislocations in garnet by PMD method.

Due to the heterogeneity of dislocation distribution, the larger the measured area is, the closer to the true value of dislocation density will be. In this study, the dislocation

Fig. 7 Schematic diagram of the premelting reaction at crystal defects in garnet. **a** Four stages of the premelting reaction at crystal defects under high temperatures. **b** The distribution and composition of the premelting lines in garnet



density of megacrystal garnet Mgc1-1 obtained by PMD is similar to that analyzed by TEM (Table 2), which indicates that the PMD is a new reliable method for revealing dislocations in garnet. Since the measured area or volume using PMD is much larger than using TEM, we infer that the data obtained by PMD is closer to the true value of dislocation density in this sample. Compared with TEM and ECCI, the PMD method is relatively simple, inexpensive and rapid. However, this method, like etch pitting, is not suitable for analyzing the sample with high dislocation densities ($> 10^8 \text{ cm}^{-2}$) due to the overlap of premelting lines.

Geological implications

The temperature for brittle–ductile transition of silicate garnet is above 850 °C ($T > 0.65 T_m$) in nature, which is so high that its dislocation pattern could reflect deformation information in the deep earth (Wang and Ji 1999). Thus, the dislocation pattern in deformed garnet is regarded as a high-temperature deformation indicator (Ji and Martignole 1994; Voegelé et al. 1998a) and a differential stress piezometer (Ando et al. 1993; Chen et al. 1996; Lü et al. 2004). The PMD method presented here could overcome the shortcomings of TEM, such as on large area and in situ analysis, and provide more reliable data on the dislocation density of garnet to relate its corresponding chemical and physical

properties, which is important for understanding the plastic deformation mechanism of garnet and the associated geodynamic process (Chen et al. 1996; Karato et al. 1995; Voegelé et al. 1998b). Since the new dislocation density piezometer of olivine has been established by Karato and Jung (2003) based on the oxidation decoration method, we can use our PMD method to recalibrate the differential stress piezometer of garnet which is established by Ando et al. (1993).

Conclusions

The PMD method provides a new approach for observing dislocation microstructures in garnet by optical microscope. Compared with TEM, this approach greatly reduces the cost and time involved in examining large areas of dislocation microstructures in garnet. This method could be used to investigate the correlations between dislocation microstructure and grain size, water content and chemical composition, and it will help to establish a more practical dislocation density differential stress piezometer.

Acknowledgements We are grateful to Prof. David L. Kohlstedt, Editor Larissa F. Dobrzinetskaya, Reviewers Jun-ichi Ando and Shun-ichi Karato and Florian Heidelbach for their valuable comments and advice. We thank Mouchun He for his technical assistance in Raman

spectroscopy analysis. This work was supported by the National Natural Science Foundation of China (Grant nos. 40872136, 41272224).

References

- Allen FM, Smith BK, Buseck PR (1987) Direct observation of dissociated dislocations in garnet. *Science* 238:1695–1697
- Alsayed AM, Islam MF, Zhang J, Collings PJ, Yodh AG (2005) Premelting at defects within bulk colloidal crystals. *Science* 309:1207–1210
- Ando J, Fujino K, Takeshita T (1993) Dislocation microstructures in naturally deformed silicate garnets. *Phys Earth Planet Inter* 80:105–116
- Aparicio C, Filip J, Skogby H, Marusak Z, Mashlan M, Zboril R (2012) Thermal behavior of almandine at temperatures up to 1200 °C in hydrogen. *Phys Chem Miner* 39:311–318
- Bartis FJ (1977) Pre-melting near crystal dislocations. *Nature* 268:427–428
- Baxter EF, Caddick MJ, Ague JJ (2013) Garnet: common mineral, uncommonly useful. *Elements* 9:415–419
- Caddick MJ, Kohn MJ (2013) Garnet: witness to the evolution of destructive plate boundaries. *Elements* 9:427–432
- Carstens H (1969) Dislocation structures in pyrope from Norwegian and Czech garnet peridotites. *Contrib Miner Petrol* 24:348–353
- Carstens H (1971) Plastic stress relaxation around solid inclusions in pyrope. *Contrib Miner Petrol* 32:289–294
- Chen J, Wang Q, Zhai M (1996) Plastic deformation of garnet in eclogites. *Sci China (D)* 39:18–25
- Cong B, Zhai M, Carswell DA, Wilson RN, Wang Q, Zhao Z, Windley BF (1995) Petrogenesis of ultrahigh-pressure rocks and their country rocks at Shuanghe in Dabie Shan, central China. *Eur J Miner* 7:119–138
- D'Ippolito V, Andreozzi GB, Bersani D, Lottici PP (2015) Raman fingerprint of chromate, aluminate and ferrite spinels. *J Raman Spectrosc* 46:1255–1264
- De Faria DLA, Lopes FN (2007) Heated goethite and natural hematite: can Raman spectroscopy be used to differentiate them? *Vib Spectrosc* 45:117–121
- De Faria DLA, Ven Ncio Silva S, de Oliveira MT (1997) Raman microspectroscopy of some iron oxides and oxyhydroxides. *J Raman Spectrosc* 28:873–878
- Doukhan N, Sautter V, Doukhan JC (1994) Ultradeep, ultramafic mantle xenoliths: transmission electron microscopy preliminary results. *Phys Earth Planet Inter* 82:195–207
- Gillet P, Fiquet G, Malezieux JM, Geiger CA (1992) High-pressure and high-temperature Raman-spectroscopy of end-member garnets—pyrope, grossular and andradite. *Eur J Miner* 4:651–664
- Gómez L, Dobry A, Geuting C, Diep HT, Burakovsky L (2003) Dislocation lines as the precursor of the melting of crystalline solids observed in Monte Carlo simulations. *Phys Rev Lett* 90:095701
- Gutierrez-Urrutia I, Raabe D (2012) Dislocation density measurement by electron channeling contrast imaging in a scanning electron microscope. *Scr Mater* 66:343–346
- Hand M, Dirks P (1992) The influence of deformation on the formation of axial-planar leucosomes and the segregation of small melt bodies within the migmatitic Napperby Gneiss, central Australia. *J Struct Geol* 14:591–604
- Hsu LC (1968) Selected phase relationships in the system Al–Mn–Fe–Si–O–H: a model for garnet equilibria. *J Petrol* 9:40–83
- Ji S, Martignole J (1994) Ductility of garnet as an indicator of extremely high-temperature deformation. *J Struct Geol* 16:985–996
- Jin Z, Zhang J, Green HW, Jin S (2001) Eclogite rheology: implications for subducted lithosphere. *Geology* 29:667–670
- Jung H, Karato S (2001) Effects of water on dynamically recrystallized grain-size of olivine. *J Struct Geol* 23:1337–1344
- Jung S, Jung H, Austrheim H (2014) Characterization of olivine fabrics and mylonite in the presence of fluid and implications for seismic anisotropy and shear localization. *Earth Planets Space* 66:1–21
- Karato S (1987) Scanning electron microscope observation of dislocations in olivine. *Phys Chem Miner* 14:245–248
- Karato S, Jung H (2003) Effects of pressure on high-temperature dislocation creep in olivine. *Philos Mag* 83:401–414
- Karato S, Wang Z, Liu B, Fujino K (1995) Plastic-deformation of garnets: systematics and implications for the rheology of the mantle transition zone. *Earth Planet Sc Lett* 130:13–30
- Keesmann I, Matthes S, Schreyer W, Seifert F (1971) Stability of almandine in the system FeO–(Fe₂O₃)–Al₂O₃–SiO₂–(H₂O) at elevated pressures. *Contrib Miner Petrol* 31:132–144
- Kleinschrodt R, McGrew A (2000) Garnet plasticity in the lower continental crust: implications for deformation mechanisms based on microstructures and SEM-electron channeling pattern analysis. *J Struct Geol* 22:795–809
- Kohlstedt DL, Goetze C, Durham WB, Sande JV (1976) New technique for decorating dislocations in olivine. *Science* 191:1045–1046
- Levine J, Mosher S, Rahl JM (2016) The role of subgrain boundaries in partial melting. *J Struct Geol* 89:181–196
- Li S, Jagoutz E, Chen Y, Li Q (2000) Sm–Nd and Rb–Sr isotopic chronology and cooling history of ultrahigh pressure metamorphic rocks and their country rocks at Shuanghe in the Dabie Mountains, Central China. *Geochim Cosmochim Acta* 64:1077–1093
- Liou JG, Zhang R, Jahn B (1997) Petrology, geochemistry and isotope data on a ultrahigh-pressure jadeite quartzite from Shuanghe, Dabie mountains, east-central China. *Lithos* 41:59–78
- Liu F, Xue H, Xu Z, Liang F, Axel G (2006) SHRIMP U–Pb zircon dating from eclogite lens in marble, Shuanghe area, Dabie UHP terrane: restriction on the prograde, UHP and retrograde metamorphic ages. *Acta Petrol Sin* 22:1761–1778
- Liu X, Xie Z, Wang L, Xu W, Jin Z (2016) Water incorporation in garnets from ultrahigh pressure eclogites at Shuanghe. *Dabie Shan Miner Mag* 80:959–975
- Lü G, Liu R, Wang F, Chen J (2004) Formation depth of coesite-bearing eclogite, Dabie UHPM zone, China. *J Earth Sci China* 15:206–215
- Massey MA, Prior DJ, Moecher DP (2011) Microstructure and crystallographic preferred orientation of polycrystalline microgarnet aggregates developed during progressive creep, recovery, and grain boundary sliding. *J Struct Geol* 33:713–730
- Mei QS, Lu K (2007) Melting and superheating of crystalline solids: from bulk to nanocrystals. *Prog Mater Sci* 52:1175–1262
- Mei S, Suzuki AM, Kohlstedt DL, Xu L (2010) Experimental investigation of the creep behavior of garnet at high temperatures and pressures. *J Earth Sci China* 21:532–540
- Meyers CE, Petuskey WT, Halloran JW, Bowen HK (1980) Phase equilibria in the system Fe–Al–O. *J Am Ceram Soc* 63:659–663
- Okay AI (1993) Petrology of a diamond and coesite-bearing terrain: Dabie Shan, China. *Eur J Miner* 5:659–675
- Prior DJ, Wheeler J, Brenker FE, Harte B, Matthews M (2000) Crystal plasticity of natural garnet: new microstructural evidence. *Geology* 28:1003–1006
- Shebanova ON, Lazor P (2003) Raman study of magnetite (Fe₃O₄): laser-induced thermal effects and oxidation. *J Raman Spectrosc* 34:845–852
- Smit MA, Scherer EE, John T, Janssen A (2011) Creep of garnet in eclogite: mechanisms and implications. *Earth Planet Sc Lett* 311:411–419
- Thibeau RJ, Brown CW, Heidersbach RH (1978) Raman spectra of possible corrosion products of iron. *Appl Spectrosc* 32:532–535

- Tumarkina E, Misra S, Burlini L, Connolly JAD (2011) An experimental study of the role of shear deformation on partial melting of a synthetic metapelite. *Tectonophysics* 503:92–99
- Verble JL (1974) Temperature-dependent light-scattering studies of the Verwey transition and electronic disorder in magnetite. *Phys Rev B* 9:5236–5248
- Voegelé V, Ando JI, Cordier P, Liebermann RC (1998a) Plastic deformation of silicate garnets I. High-pressure experiments. *Phys Earth Planet Inter* 108:305–318
- Voegelé V, Cordier P, Sautter V, Sharp TG, Lardeaux JM, Marques FO (1998b) Plastic deformation of silicate garnets II. Deformation microstructures in natural samples. *Phys Earth Planet Inter* 108:319–338
- Wang Z, Ji S (1999) Deformation of silicate garnets: Brittle–Ductile transition and its geological implications. *Can Miner* 37:525–541
- Xie Z, Liu X, Jin Z (2018) Effect of water on the dislocation mobility in garnet: evidence from the Shuanghe UHP eclogites, Dabie orogen, China. *Tectonophysics* (**Under review**)
- Xu L, Mei S, Dixon N, Jin Z, Suzuki AM, Kohlstedt DL (2013) Effect of water on rheological properties of garnet at high temperatures and pressures. *Earth Planet Sci Lett* 379:158–165
- Yamamoto T, Ando J, Tomioka N, Kobayashi T (2017) Deformation history of Pinatubo peridotite xenoliths: constraints from microstructural observation and determination of olivine slip systems. *Phys Chem Miner* 44:247–262
- Zhang JL, Zaefferer S, Raabe D (2015) A study on the geometry of dislocation patterns in the surrounding of nanoindenters in a TWIP steel using electron channeling contrast imaging and discrete dislocation dynamics simulations. *Mater Sci Eng A* 636:231–242